Combined Importance Sampling and Separable Monte Carlo: Analytical Variance Estimator and applications to Structural Reliability

Gabriele Capasso, Christian Gogu, Christian Bes, Jean-Philippe Navarro, Martin Kempeneers

Combined Importance Sampling and Separable Monte Carlo: Analytical Variance Estimator and applications to Structural Reliability

August 29, 2022

Abstract

This paper considers reliability analysis problems where the limit state function, characterizing the failure domain, can be expressed in terms of two independent components: response and capacity. An approach called Separable Importance Sampling has been proposed in the literature as an extension of Importance Sampling, allowing improved sampling efficiency due to separable sampling of response and capacity. In this paper we derive a new analytical variance estimator for the probability of failure estimated by Separable Importance Sampling, allowing to analytically determine the number of samples required to reach a given coefficient of variation on the probability of failure. Numerical investigations have been conducted on two benchmark reliability problems. Thanks to this variance estimator we were able to carry out a large number of numerical experiments, allowing us to provide a comprehensive analysis of situations where Separable Importance Sampling would be most beneficial.

Keywords *reliability analysis; structural reliability; separable limit state; Monte Carlo methods; separable Monte Carlo; importance sampling; sampling methods; analytical variance estimator*

1 Introduction

In recent decades, probabilistic design approaches gained a growing interest in both the scientific community and in industry. Uncertainties in input data can be analyzed in a rational framework to measure the impact on outputs, determine the most influential factors on output variability, accredit a model, verify the compliance of prerequisites imposed by legislation or select the best design [De Rocquigny et al. (2008)]. Reliability analyses focus on ascertaining the failure risk associated to a specific engineering design [Larsson (2015)]. Over the past decades, the paradigms of this field have been progressively formalized [Pham (2006), Rykov et al. (2010), Birolini (2013), Trivedi & Bobbio (2017)].

Such concepts are applied in almost all knowledge fields, from medicine, finance [Rykov et al. (2010)], engineering systems [Rausand & Høyland (2003)] to automotive, aerospace and ship industry [Nikolaidis et al. (2007)]. In this article, particular attention is given to structural reliability applications [Lemaire (2013), Gogu (2021)].

To assess the reliability level of a designed structure, several metrics were introduced in the literature. The most common is the index β_{HL} introduced by Hasofer and Lind [Hasofer & Lind (1974)], which is defined as the minimum Euclidean distance (L^2 norm) between origin of a standard normal space and the Limit State Surface (LSS) representing a failure mode of the system. The point situated at distance β_{HL} is known as *design point* or *Most Probable Failure Point* (*MPFP*).

Another important reliability performance metric is given by the failure probability P_f. The classical Monte Carlo (MC) simulation method is probably among the simplest and most popular sampling based simulation methods used in reliability applications [Hammersley (2013)] to determine P_f. Originally defined to compute general integrals, it simply consists in sampling data according to the input distributions and estimating the expectation trough an arithmetic sum. This constitutes the reference for all successive approaches, because of its simplicity, intrinsic stability and independence from problem dimension and complexity of the system considered in the analysis.

On the downsides, MC presents a slow convergence rate, above all for rare events estimation. This led to the need for more agile methods, able to reduce the variance of the P_f estimation with the same number of samples.

Importance Sampling (IS), another popular variance reduction technique Tokdar & Kass (2010), is based on the concentration of the sampling in specific areas defined by a support distribution. While IS has been initially developed in the context of reliability several decades ago, it continues to be a very active topic with many recent developments seeking to further improve it [Papaioannou et al. (2019), Chaudhuri et al. (2020), Nadjafi & Najafi ARK (2021), Tabandeh et al. (2022)], together with industrial applications, like [Gao et al. (2020), Misraji et al. (2020), Saaed & Daghigh (2021), Liu et al. (2022), Subramanian & Mahadevan (2022)] among others. One open problem is given by the most efficient construction of the support importance distribution of IS. Several advanced techniques, going by the name of Adaptive Importance Sampling, build this importance function during the simulations in an adaptive way [Karamchandani et al. (1989), Zhang (1996), Au & Beck (1999), Richard & Zhang (2007), Cappé et al. (2008), Müller et al. (2019), Zhang et al. (2022)]. This issue is not specifically considered in the present article, but needs to be kept in mind.

Another variance reduction technique, Separable Monte Carlo (SMC) [Smarslok (2009), Smarslok et al. (2010)] focuses on a particular category of limit state functions, where response and capacity (typically stress and strength in structural analysis) present no mutual dependence (or simply rely on distinct independent input variables). This assumption is common in structural engineering [Smarslok (2009)]. This consists in sampling stress and strength (or response

and capacity, as denoted in [Smarslok et al. (2010)]) separately and evaluate every possible combination of the two. Therefore, a larger database could be built with fewer simulations, while also allowing the construction of unbalanced datasets to exploit differences in computational burden of response and capacity (the latter is usually computationally inexpensive to sample).

Following the same idea, Importance Separable Monte Carlo (ImpSMC) was also proposed by [Chaudhuri & Haftka (2013)]. This is in fact a combination of IS and SMC, benefiting from the respective advantages of both approaches. In [Chaudhuri & Haftka (2013)], a failure probability estimator was presented, and the resulting variance reduction was illustrated empirically. Unfortunately, to date no closed form expression of the variance of the P_f estimated by ImpSMC is available. This shortcoming makes it difficult to optimally exploit the method in order to achieve maximum numerical efficiency gains. Thus, the objective of this article is to develop a closed form variance estimator of the P_f estimated by ImpSMC and to extensively analyze situations in which the ImpSMC procedure will be most useful.

In Section 2 a brief overview of MC, IS and SMC is provided. In Section 3, ImpSMC approach is presented and essentials of the proposed variance estimator proof are reported. Two numerical examples, related to two structural reliability test cases, are presented in Section 4 to compare methods enunciated in Sections 2 and 3. Then, conclusions are summarized in Section 6. For the interested reader, empirical variance validation and further details of variance estimator proof are reported in the Appendix.

2 Background on relevant sampling-based methods

The goal of this section is to present several approaches adopted to evaluate the failure probability of a system. We are going to use the following notation:

- X: random design variable;
- x: realization of X;
- $g(X)$: Limit State Function (LSF), conventionally negative to indicate a failure state;
- $G(X) = 1_{g(X)<0}$: failure indicator.

The LSF is expressed in a way that it is negative when the system is in a failure condition. The hypersurface described by $g(X) = 0$ is often referred as Limit State Surface (LSS).

2.1 Monte Carlo (MC) Simulation

MC is usually considered as a reference for all sampling-based reliability approaches. In integral form, the failure probability can be expressed as follows:

$$P_f = \int_D G(x) f(x) dx \tag{1}$$

Here f represents the Probability Density Function (PDF) of the random variable X. Denoting by $\widehat{P_f}$ an estimator of P_f, expectation, variance and coefficient of variation coV of this estimator are reported in the following equations:

$$E\left[\widehat{P_f}\right] \approx \frac{1}{N}\sum_{i=1}^{N} G(x_i) \qquad Var(\widehat{P_f}) \approx \frac{E\left[\widehat{P_f}\right] - E\left[\widehat{P_f}\right]^2}{N} \qquad coV(\widehat{P_f}) \approx \sqrt{\frac{1 - E\left[\widehat{P_f}\right]}{NE\left[\widehat{P_f}\right]}} \tag{2}$$

Generally, coV is the performance indicator adopted to indicate the precision of the estimation itself. It is easy to understand that MC is not affected by the curse of dimensionality of the problem. Moreover, it is stable and makes no assumption on the LSS itself. However, for rare event estimation, the convergence rate of coV follows $(P_f N)^{-1/2}$, leading to a very high number of simulations necessary to achieve an acceptable precision.

2.2 Importance Sampling (IS)

Importance Sampling is a well-known approach to estimate integrals with fewer data than MC. It stems from a very simple operation on the P_f integral:

$$P_f = \int_D G(x) f(x) dx = \int_D G(x) f(x) \frac{q(x)}{q(x)} dx = \int_D \left(G(x) \frac{f(x)}{q(x)} \right) q(x) dx \tag{3}$$

Here q represents a generic function, which must only respect the requirement of being equal to zero where $f(x) = 0$. In particular, in IS the function q is a PDF constituting the support importance function. Therefore, x realizations of the random variable X are sampled following the PDF q. In a compact notation, Eq. 3 can be rewritten as follows:

$$P_f = E_q\left[G(X)w(X)\right] \qquad w(X) = \frac{f(X)}{q(X)} \quad X \sim q \tag{4}$$

The quantity w is often referred in the literature as *importance weight*. Expectation and variance of the corresponding P_f estimator are reported in the following equation:

$$E\left[\widehat{P_f}\right] \approx \frac{1}{N}\sum_{i=1}^{N} G(x_i)w(x_i) \qquad Var(\widehat{P_f}) \approx \frac{1}{N}\sum_{i=1}^{N} \left[G(x_i)w(x_i) - E\left[\widehat{P_f}\right]\right]^2 \tag{5}$$

2.3 Separable Monte Carlo (SMC)

The Separable Monte Carlo (SMC) method, proposed by Smarslok et al. [Smarslok (2009), Smarslok et al. (2010)], was initially developed in a structural reliability context but it is generalizable to any reliability problem, under an independence assumption. In structural reliability, the method starts from the assumption that strength R and stress S rely on distinct independent variables. The key feature behind SMC is the possibility to sample separately R and S, and successively compare all combinations of their respective instances.

In this context the LSF is expressed as follows:

$$g(X) = g(X_R, X_S) = R(X_R) - S(X_S) \tag{6}$$

Where X_R and X_S are partitions of the original design variable vector X affecting either capacity R or response S respectively. Random variables X_R and X_S are considered to be independent. Such an independence assumption is often verified in structural reliability but it can, of course, be verified in a large number of other applications. The failure indicator G is rewritten in compact notation as follows:

$$G(R, S) = 1_{R<S} = I(R < S) \tag{7}$$

Here we omit the fact that response and capacity are actually functions of original variable sets X_R and X_S (i.e. $R = R(X_R)$ and $S = S(X_S)$) in order not to overload the notation. Of course, input variables X_R and X_S are sampled according to their original distributions while R and S are computed as output. This does not affect neither results nor the proof. It is worth noticing that the expressions in Eqs. 6-7 are mere examples of separation between two blocks R and S: since the proof for the SMC procedure [Smarslok et al. (2010)] does not require a particular choice on the expression of g, the validity is actually extended to any LSF defined by any operation linking two independent variables. Denoting by r and s realizations of respectively R and S, and by D_R and D_S their domains, failure probability can be expressed as:

$$P_f = \int_D G(r, s) f_{RS}(r, s) dr ds = \int_{D_S} f_S(s) \left(\int_{D_R} G(r, s) f_R(r) dr \right) ds \tag{8}$$

Using a compact notation, expectation will be given by:

$$P_f = E_S \left[E_R \left[\widetilde{F_R}(S) \right] \right] \quad \text{where } \widetilde{F_R}(S) = G(R, S) \tag{9}$$

The choice of the symbol $\widetilde{F_R}(S)$ is justified by the fact that its expectation with respect to the capacity variable is the conditional CDF F_R of the variable R at point S [Smarslok et al. (2010)]. Failure probability estimation will therefore be given by [Smarslok et al. (2010)]:

$$E\left[\widehat{P_f}\right] \approx \frac{1}{NM} \sum_{i=1}^{N} \sum_{j=1}^{M} G\left(r_j, s_i\right) \tag{10}$$

A variance estimator can be expressed as follows (proof available in [Smarslok (2009)]):

$$Var(\widehat{P_f}) = \frac{1}{NM}P_f + \frac{M-1}{NM}E_S\left[E_R\left[\widetilde{F_R}(S)\right]^2\right] + \frac{N-1}{MN}E_S\left[E_R\left[\widetilde{F}(\min(S_1,S_2))\right]\right] - \frac{N+M-1}{NM}P_f^2 \tag{11}$$

The numerical quantities can be obtained trough the following approximations:

$$\begin{aligned} E_S\left[E_R\left[\widetilde{F_R}(S)\right]^2\right] &\approx \frac{1}{N}\sum_{i=1}^{N}\left(\sum_{j=1}^{M}\frac{G(r_j,s_i)}{M}\right)^2 \\ E_S\left[E_R\left[\widetilde{F_R}(S_1),\widetilde{F_R}(S_2)\right]\right] &\approx \frac{2}{NM}\sum_{i=1}^{N/2}\sum_{j=1}^{M}(G(r_j,s_{2i-1})G(r_j,s_{2i})) \end{aligned} \tag{12}$$

The term $G(r_j, s_{2i-1})G(r_j, s_{2i})$ was reported in the original work Smarslok et al. (2010) as $G(r_j, \min(s_{2i-1}, s_{2i}))$, since the main focus was on LSF expressed as in Eq. 6. However, the proof of the analytical variance estimator is not affected by the choice of the shape of g (and thus G) function, but only requires a separation between two independent blocks R and S, thus we propose to use the more general notation in Eq. 12.

Separate sampling of R and S allows to create a larger database with fewer simulations of each. Moreover, when capacity and response simulations imply very different computational burdens (often sampling S is much more costly), one can use unbalanced datasets, reducing the overall computational efforts. On top of that, a significant variance reduction with respect to MC was shown in [Smarslok et al. (2010)]. In particular, SMC proved to be increasingly beneficial when most of LSF variance came from capacity [Smarslok (2009)].

3 ImpSMC approach

This section provides a full description of the method known as *ImpSMC* (Importance Separable Monte Carlo), introduced by [Chaudhuri & Haftka (2013)]. This method consists of a combination of the upper-mentioned *IS* and *SMC*, and it is the method for which we will seek to construct a variance estimator for its probability of failure estimate.

3.1 Probability of failure estimation

As for *SMC*, R and S are functions of original variable sets X_R and X_S. To improve readability, this dependence is omitted, while keeping in mind that the

actual sampling is performed on X_R and X_S. These are sampled according to support functions (or importance distributions) respectively $q(X_R)$ et $h(X_S)$. In the following, response and capacity will be treated as the sampled variables and importance distributions will be denoted as $q(R)$ and $h(S)$, without this affecting results. Repeating the same processes used for *IS* and *SMC*, one obtains:

$$P_f = E_h\left[\frac{f_S(S)}{h(S)} E_q\left[\frac{G(R,S) f_R(R)}{q(R)} \mid S\right]\right] \tag{13}$$

In the following, a compact notation, consistent with Smarslok et al. (2010), is adopted:

$$\begin{aligned}
\widetilde{H}_R(S) = \widetilde{H}(R,S) &= \frac{f_S(S)}{h(S)} \frac{f_R(R)}{q(R)} G(R,S) \\
\widehat{H}_R(S) &= \frac{1}{M} \sum_{j=1}^{M} \widetilde{H}(R_j, S) \\
H(S) &= E_q[\widehat{H}_R(S)|S] = E_q[\widetilde{H}_R(S)|S] \\
\widehat{P_f} &= \frac{1}{N} \sum_{i=1}^{N} \widehat{H}_R(S_i) \\
P_f &= E_h\left[E_q[\widetilde{H}_R(S)|S]\right] = E_h[H(S)] = E\left[\widehat{P_f}\right]
\end{aligned} \tag{14}$$

Here the subscript R implies a dependence of $\widetilde{H}$ with respect to R variable and must not be confused with q and h representing the two importance functions used to sample R and S variables respectively. As for *SMC*, when estimating P_f based on samples according to Eq. 13, all possible combinations of R and S are compared to each other to verify a failure condition. We take this into account by introducing N independent identically distributed copies of S in our estimation. We make the distinction between the original variable $\widetilde{H_R}$ and its estimation $\widehat{H_R}$ via arithmetic mean.

The corresponding probability of failure estimator will be given by:

$$E\left[\widehat{P_f}\right] \approx \frac{1}{NM} \sum_{i=1}^{N} \sum_{j=1}^{M} G\left(r_j, s_i\right) \frac{f_R(r_j)}{q(r_j)} \frac{f_S(s_i)}{h(s_i)} \tag{15}$$

Where M represents the number of realizations of the capacity R.

3.2 Variance estimation on $\widehat{P_f}$

The novelty proposed in the present article consists in the determination of an analytical variance estimator. In Chaudhuri & Haftka (2013), variance reduction was proved empirically, but no actual theoretical estimator of the associated variance was provided.

We focus on the definition of the analytical estimator of $Var(\widehat{P_f})$, starting from Eq. 14. It is worth noticing that even though all S_i are independent, the terms $\widehat{H}_R(S_i)$ are not. Therefore, a correlation in datasets is present and a covariance term will appear in the variance of the sum over all terms defined by the copies of the variable S:

$$Var(\widehat{P_f}) = \frac{1}{N^2}\left(\sum_{i=1}^{N} Var[\widehat{H}_R(S_i)] + 2\sum_{i=1}^{N}\sum_{j=i+1}^{N} Cov[\widehat{H}_R(S_i), \widehat{H}_R(S_j)]\right)$$

Here, the variable R is unique and thus is not indexed in the sum (the notation $\widehat{H}_R(S)$ clarifies the concept). Since all S_i and S_j are independent identically distributed random variables according to S, one may obtain:

$$Var(\widehat{P_f}) = \frac{1}{N} Var[\widehat{H}_R(S)] + \frac{N-1}{N} Cov[\widehat{H}_R(S_1), \widehat{H}_R(S_2)] \tag{16}$$

It is important to underline the fact that all samples of R are combined with all samples of S. We do not simply assign M different samples to each of the N samples of S: this would lead to use NM samples of R, as in conditional expectation method, and the variance term of Eq. 16 would be sufficient. If we arrange the values of $\widetilde{H}(R_j, S_i)$ in a 2D matrix, this re-use of the same samples induces a correlation between the results in the same row (respectively column). Given the need for a covariance term describing such correlation, we start the proof from the covariance estimation at a fixed point (which will be necessary to easily compute both variance and covariance terms).

The first step aims at determining the covariance between two values of $\widehat{H}_R$ at two fixed points t_1 and t_2. After several manipulations one may obtain:

$$Cov_q\left[\widehat{H}_R(t_1), \widehat{H}_R(t_2)\right] = \frac{1}{M}\left(E_q\left[\widetilde{H}_R(t_1)\widetilde{H}_R(t_2)\right] - H(t_1)H(t_2)\right) \tag{17}$$

In the second step, the total variance law allows to write:

$$Var(\widehat{H}_R(S)) = E_h\left[Var_q(\widehat{H}_R(S)|S)\right] + Var_h\left[E_q(\widehat{H}_R(S)|S)\right] \tag{18}$$

The first term can be treated as the conditional covariance of $\widehat{H}_R(S)$ on itself:

$$\begin{aligned} E_h\left[Var_q(\widehat{H}_R(S)|S)\right] &= E_h\left[Cov_q(\widehat{H}_R(S)|S, \widehat{H}_R(S)|S)\right] \\ &= \frac{1}{M}\left(E_h\left[E_q\left[\widetilde{H}_R^2(S)\right]\right] - E_h\left[H^2(S)\right]\right) \end{aligned} \tag{19}$$

Then the second term:

$$Var_h\left[E_q(\widehat{H}_R(S)|S)\right] = E_h\left[E_q\left[\widetilde{H}_R(S)\right]^2\right] - E_h\left[E_q\left[\widetilde{H}_R(S)\right]\right]^2 = E_h\left[H^2(S)\right] - P_f^2 \tag{20}$$

To determine the covariance part in Eq. 16, one has to start from the total covariance theorem:

$$Cov(X_1, X_2) = E_Y\left[Cov_{X_1,X_2}(X_1, X_2|Y)\right] + Cov_Y\left[E_{X_1}(X_1|Y), E_{X_2}(X_2|Y)\right] \tag{21}$$

In this case, the different variables in Eq. 21 are given by the tern:

$$X_1 = \widehat{H}_R(S_1), \quad X_2 = \widehat{H}_R(S_2), \quad Y = (S_1, S_2)$$

The term Cov_Y in Eq. 21 can be neglected as S_1 and S_2 are, by definition, independent copies of S. The only remaining part can be developed by using the fixed point covariance equation (see Eq. 17):

$$Cov_{\widehat{H}_R(S_1),\widehat{H}_R(S_2)}\left(\widehat{H}_R(S_1), \widehat{H}_R(S_2)|S_1, S_2\right) = \frac{1}{M}\left(E_q\left[\widetilde{H}_R(S_1)\widetilde{H}_R(S_2)\right] - H(S_1)H(S_2)\right)$$

Passing to the expectation, it is worth noticing that, since $H(S_1)$ and $H(S_2)$ are independent (as they are functions of S_1 and S_2 which are independent by definition), we obtain:

$$E_h\left[H(S_1)H(S_2)\right] = E_h\left[H(S_1)\right]E_h\left[H(S_2)\right] = P_f^2$$

Therefore, one may obtain the following relation:

$$Cov(\widehat{H}_R(S_1), \widehat{H}_R(S_2)) = \frac{1}{M}\left(E_h\left[E_q\left[\widetilde{H}_R(S_1)\widetilde{H}_R(S_2)\right]\right] - P_f^2\right) \tag{22}$$

Now, joining together results from Eqs. 19,20 and 22 and substituting in Eq. 16, the final analytical covariance estimator is obtained:

$$\begin{aligned} Var(\widehat{P_f}) = &\frac{1}{NM}E_h\left[E_q\left[\widetilde{H}_R^2(S)\right]\right] + \frac{M-1}{NM}E_h\left[H^2(S)\right] + \frac{N-1}{MN}E_h\left[E_q\left[\widetilde{H}_R(S_1)\widetilde{H}_R(S_2)\right]\right] \\ &- \frac{N+M-1}{NM}P_f^2 \end{aligned} \tag{23}$$

Re-writing this expression in a more compact way, one may retrieve:

$$Var(\widehat{P_f}) = \frac{1}{NM}\phi_1 + \frac{1}{N}\phi_2 + \frac{N-1}{NM}\xi_{12} \tag{24}$$

Where:

$$\begin{aligned} \phi_1 &= E_h\left[E_q\left[\widetilde{H}_R^2(S)\right]\right] - E_h\left[H^2(S)\right] \\ \phi_2 &= E_h\left[H^2(S)\right] - P_f^2 \\ \xi_{12} &= E_h\left[E_q\left[\widetilde{H}_R(S_1)\widetilde{H}_R(S_2)\right]\right] - P_f^2 \end{aligned} \tag{25}$$

The effect of the covariance term on the overall variance of the estimation of P_f via ImpSMC is measured by ξ_{12}, while the terms ϕ_1 (second order effect) and ϕ_2 represent the influence of the variance term. The numerical estimation of the variance obtained in Eq. 24 thus needs the following ingredients:

$$\begin{aligned}
\widetilde{T}_{j,i} &= G\left(R_j, S_i\right) \frac{f_R(r_j)}{q(r_j)} \frac{f_S(s_i)}{h(s_i)} \\
P_f = E_h\left[E_q\left[\widetilde{H}_R(S)\right]\right] &\approx \frac{1}{NM} \sum_{i=1}^{N} \sum_{j=1}^{M} \widetilde{T}_{j,i} \\
E_h\left[E_q\left[\widetilde{H}_R(S)^2\right]\right] &\approx \frac{1}{NM} \sum_{i=1}^{N} \sum_{j=1}^{M} \widetilde{T}_{j,i}^2 \\
E_h\left[H^2(S)\right] = E_h\left[E_q\left[\widetilde{H}_R(S)\right]^2\right] &\approx \frac{1}{N} \sum_{i=1}^{N} \left(\sum_{j=1}^{M} \frac{\widetilde{T}_{j,i}}{M} \right)^2 \\
E_h\left[E_q\left[\widetilde{H}_R(S_1), \widetilde{H}_R(S_2)\right]\right] &\approx \frac{2}{NM} \sum_{i=1}^{N/2} \sum_{j=1}^{M} \left(\widetilde{T}_{j,2i-1} \widetilde{T}_{j,2i} \right)
\end{aligned} \tag{26}$$

It is possible to verify that from Eqs. 23 and 26 one can retrieve Eqs. 11 and 12 for SMC.

3.3 Variance estimator potential

The closed form variance estimator of P_f estimated by ImpSMC makes it possible to completely exploit the ImpSMC approach, as it allows to:

- evaluate variability of P_f without having to reproduce the reliability analysis several times;
- stop sampling when a fixed accuracy target on P_f estimation is reached;
- preliminarily estimate the minimum number M of R samples (respectively N for S) necessary to achieve the accuracy goal;
- preview the number M_k of R (respectively N_k of S) samples needed to reach targeted variance $\overline{Var}$, given a fixed ratio $k = N/M$;
- a priori determine the ratio N/M between number of samples of S and R allowing to minimize global computational burden.

The first two advantages of such variance estimator are straight-forward. For preliminary evaluation purposes, it is possible to exploit outcomes in Eq. 24 by determining all terms in Eq. 26 with few simulations, say $N = M = 100$. Then, under the assumptions that those latter do not significantly change with an increase in number of samples nor with variation in ratio k, Eq. 24 can be used to preview all the relations between precision and number of samples.

This can be represented on a contour plot, graphically illustrating the levels of $coV(\widehat{P_f})$ as a function of N and M, as done in Smarslok (2009), Smarslok et al. (2010) for SMC. The asymptotic behaviors can be extracted from quantities in Eq. 25:

$$\min N = \frac{\phi_2}{\overline{Var}} \qquad \min M = \frac{\xi_{12}}{\overline{Var}} \qquad k^* = \arg\min_k N_k M_k = \frac{\phi_2}{\xi_{12}} \tag{27}$$

A particular remark can be done about the ratio k allowing to minimize the product NM: this does not depend on the targeted $\overline{Var}$, but just relies on the nature of the model and input variabilities, namely through the terms ϕ_2 and ξ_{12}. Such ratio is not necessarily optimal in terms of computational costs as minimizing the product NM does not necessarily imply reducing the overall computational burden. In the following, we are referring to it as the *reference ratio*, individuating the ratio which is exactly mid-way between two asymptotic behaviors.

4 Numerical results

In this Section, two test cases are introduced to investigate the gain in terms of number of simulations needed to achieve a target coV, arbitrarily fixed (for the examples presented in this paper) at 0.05. In particular, in the first application a comparative analysis between two *LSF* formulations is reported, while in the second use case we conducted a study on the effects of the ratio between variances due to response and capacity components.

4.1 Composite plate test case

As a first example, a cross-ply composite plate deflection problem was considered, which was also used in [Smarslok et al. (2010), Chaudhuri & Haftka (2013)]. We focus on maximum deflection, at the middle point of a simply supported squared cross-ply plate, characterized by a $[90, 45, -45]_{sym}$ laminate with lamina thickness of 125 μm. This test case is illustrated in Fig. 1. We consider the loading condition to be a sinusoidally varying pressure, defined as:

$$q(x, y) = q_0 \sin\left(\frac{\pi x}{L}\right) \sin\left(\frac{\pi y}{L}\right)$$

Where q_0 represents the amplitude and L the length of each side of the square plate. The deflection output w is defined as:

$$w = \frac{q_0 L^4}{D^*} \qquad D^* = \pi^4 \left[D_{11} + 2\left(D_{12} + D_{66}\right) + D_{22}\right] \tag{28}$$

Here the terms D_{ij} represent the components of the bending stiffness matrix of the plate. Overall, 7 random variables (listed in Table 1) are introduced.

This part of the analysis aims at evaluating the effect of the ratio between variances of capacity and response variables (respectively R and S). To this

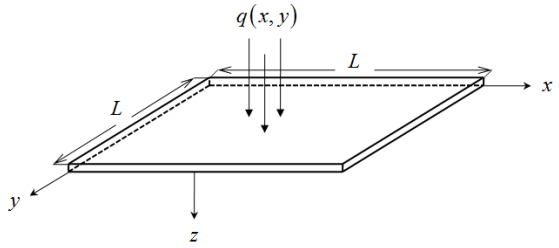

Figure 1: Cross-ply test case: illustration (Source: [Smarslok et al. (2010), Chaudhuri & Haftka (2013)])

Variable	Unit	Distribution	Mean	St. Deviation
E_1	Pa	Normal	1.5×10^{11}	7.5×10^{9}
E_2	Pa	Normal	9×10^{9}	4.5×10^{8}
G_{12}	Pa	Normal	4.6×10^{9}	2.3×10^{8}
ν_{12}		Normal	0.34	0.017
L	m	Normal	7.5×10^{-2}	1.5×10^{-3}
q_0	Pa	Normal	1.30×10^{5}	1.95×10^{4}
w_{all}	m	Log-Normal	8×10^{-3}	2.4×10^{-4}

Table 1: Cross-ply test case: random variables

purpose, in analogy with works from Smarslok (2009), Smarslok et al. (2010), two different formulations of LSF are introduced:

$$R = w_{all} \qquad S = \frac{q_0 L^4}{D^*} \tag{29a}$$

$$R = \frac{w_{all}}{q_0} \qquad S = \frac{L^4}{D^*} \tag{29b}$$

In particular, the variable sets X_R and X_S are changed, providing a higher variance to capacity variable R (respectively lower variance to response S) according to Eq. 29a to Eq. 29b. To improve readability, in the following we will refer to Eq. 29a as *Low R-Variability Formulation* (LRVF) and to Eq. 29b as *High R-Variability Formulation* (HRVF).

The analytical variance estimator described in Section 3 is empirically validated on both LSF formulations of this first test case. The empirical validation is carried out with 10^4 repeated ImpSMC analyses with $N = 10^3$ response samples and $M = 10^3, 10^4, 10^5$ capacity samples for each one. Error is measured as follows:

$$Err(P_f) = \frac{\sigma_{an}(P_f) - \sigma_{emp}(P_f)}{\sigma_{emp}(P_f)} \times 100$$

Where σ_{an} is the standard deviation predicted by analytical estimators from Eqs. 24-26 and σ_{emp} the empirical one estimated based on the 10^4 repetitions

of ImpSMC. The results, reported in Table 2, show that the maximum error is around 1%.

ID	M/N=1			M/N=10			M/N=100		
	$\sigma_{emp}(P_f)$	$\sigma_{an}(P_f)$	$Err(P_f)(\%)$	$\sigma_{emp}(P_f)$	$\sigma_{an}(P_f)$	$Err(P_f)(\%)$	$\sigma_{emp}(P_f)$	$\sigma_{an}(P_f)$	$Err(P_f)(\%)$
LRVF	2.312×10^{-4}	2.310×10^{-4}	-0.09	2.303×10^{-4}	2.306×10^{-4}	0.13	2.303×10^{-4}	2.305×10^{-4}	0.09
HRVF	1.323×10^{-4}	1.319×10^{-4}	-0.29	7.699×10^{-5}	7.619×10^{-5}	-1.04	6.842×10^{-5}	6.822×10^{-5}	-0.30

Table 2: Composite plate test case: validation of analytical variance estimator ($N = 10^3$, values issued from 10^5 repetitions)

Reliability simulation results are reported in Table 3 for *LRVF* and Table 4 for *HRVF*. The first three columns in both tables represent the mean of P_f estimations, the mean and the standard deviation of required N to achieve $coV(\widehat{P_f}) = 0.05$. The successive ones report standard deviation and coefficient of variation of P_f estimation at fixed number N of S samples ($N = 100$ in 4th and 5th columns, $N = 1000$ in 6th and 7th columns). All values are obtained by repeating 100 times the reliability analyses.

For both formulations, ImpSMC outperforms MC, IS and SMC: both $\sigma(\widehat{P_f})$ and N to reach $coV(\widehat{P_f}) = 0.05$ are noticably reduced.

In the *LRVF* case, the introduction of a separate sampling process appears more efficient when IS concept is applied: this can be observed by comparing gains allowed by ImpSMC with respect to IS (N reduced by 52%) and gains of SMC with respect to MC (N reduced by 30%). Here the ratio M/N appears to present no substantial advantage for neither SMC nor ImpSMC approach.

Looking at the *HRVF* results, improvement ratios increase for both ImpSMC and SMC with respect to IS and MC respectively. Still, ImpSMC introduces gains with respect to IS which are superior to the ones ensured by the transition from MC to SMC. Moreover, in this case the ratio M/N has a significant influence on reducing both variance of failure probability and number of required samples. In particular, creating an unbalanced dataset with more R samples, can reduce the substantial number of S samples, which usually determine most of overall computational burden.

For both formulations, IS outperforms SMC and MC: therefore, in the following, IS approach will be used as a reference for comparison.

		Results at $coV(\widehat{P_f}) = 0.05$			**Results at** $N = 100$		**Results at** $N = 1000$	
		$\widehat{P_f}$	$\overline{N}$	$\sigma_N(\%)$	$\sigma(\widehat{P_f})$	$coV(\widehat{P_f})$	$\sigma(\widehat{P_f})$	$coV(\widehat{P_f})$
MC		6.23×10^{-3}	6.4×10^4	4.45	7.36×10^{-3}	1.18	2.17×10^{-3}	0.35
IS		6.22×10^{-3}	1159	5.18	1.02×10^{-3}	0.16	2.90×10^{-4}	0.047
SMC	**M/N=1**	6.20×10^{-3}	4.5×10^4	3.35	7.21×10^{-3}	1.16	2.05×10^{-3}	0.33
	M/N=10	6.20×10^{-3}	4.4×10^4	4.37	6.95×10^{-3}	1.12	2.00×10^{-3}	0.32
	M/N=100	6.20×10^{-3}	4.4×10^4	2.42	6.41×10^{-3}	1.03	1.92×10^{-3}	0.31
ImpSMC	**M/N=1**	6.26×10^{-3}	552	7.39	7.58×10^{-4}	0.121	2.31×10^{-4}	0.037
	M/N=10	6.24×10^{-3}	549	7.10	7.46×10^{-4}	0.120	2.30×10^{-4}	0.037
	M/N=100	6.23×10^{-3}	547	6.95	7.07×10^{-4}	0.113	2.30×10^{-4}	0.037

Table 3: Composite plate: main results for *LRVF* from Eq. 29a (values issued from 100 repetitions of each reliability algorithm)

		Results at $coV(\widehat{P_f}) = 0.05$			Results at $N = 100$		Results at $N = 1000$	
		$\widehat{P_f}$	$\overline{N}$	$\sigma_N(\%)$	$\sigma(\widehat{P_f})$	$coV(\widehat{P_f})$	$\sigma(\widehat{P_f})$	$coV(\widehat{P_f})$
MC		6.23×10^{-3}	6.4×10^4	4.45	7.36×10^{-3}	1.18	2.17×10^{-3}	0.35
IS		6.26×10^{-3}	1143	11.5	1.03×10^{-3}	0.16	2.90×10^{-4}	0.046
SMC	**M/N=1**	6.24×10^{-3}	1.4×10^4	5.09	$2.68 - 3$	0.43	8.01×10^{-4}	0.13
	M/N=10	6.29×10^{-3}	4105	9.74	1.71×10^{-3}	0.27	6.20×10^{-4}	0.099
	M/N=100	6.22×10^{-3}	2985	20.2	1.47×10^{-3}	0.24	5.88×10^{-4}	0.095
ImpSMC	**M/N=1**	6.28×10^{-3}	178	35.7	3.11×10^{-4}	0.054	1.32×10^{-4}	0.021
	M/N=10	6.24×10^{-3}	59	30.5	2.37×10^{-4}	0.038	7.62×10^{-5}	0.012
	M/N=100	6.25×10^{-3}	51	23.5	2.35×10^{-4}	0.038	6.82×10^{-5}	0.011

Table 4: Composite plate: main results for *HRVF* from Eq. 29b (values issued from 100 repetitions of each reliability algorithm)

Exploiting the potentialities of the variance estimator at a higher level, it is possible to trace the evolution of coV as a function of both N and M, thanks to the algorithm described in Section 3.3. The ingredients which must be computed are ϕ_1, ϕ_2 and ξ_{12}. These are evaluated through the numerical estimators presented in Eqs. 25-26. In this part, we aim to analyze both magnitude and precision of the estimation provided for each of the extrapolation parameters ϕ_1, ϕ_2 and ξ_{12}. Numerical estimations are performed with 100 repetitions of the dataset containing $N = 100$ response (S) samples. Both LSF formulations and three different M/N ratios are investigated. Results of such estimations are summarized in Table 5.

Parameter	**Sample size**	**LRVF**		**HRVF**	
		Mean	**St. Dev. (%)**	**Mean**	**St. Dev. (%)**
ϕ_1	M/N=1	5.88×10^{-5}	4.85	1.08×10^{-4}	1.51
	M/N=10	5.87×10^{-5}	4.66	1.08×10^{-4}	1.08
	M/N=100	5.88×10^{-5}	4.54	1.08×10^{-4}	1.02
ϕ_2	M/N=1	5.32×10^{-5}	3.98	4.62×10^{-6}	11.92
	M/N=10	5.31×10^{-5}	3.58	4.53×10^{-6}	5.82
	M/N=100	5.31×10^{-5}	3.65	4.53×10^{-6}	4.87
ξ_{12}	M/N=1	2.63×10^{-7}	50.77	1.27×10^{-5}	5.08
	M/N=10	2.62×10^{-7}	49.62	1.27×10^{-5}	4.82
	M/N=100	2.64×10^{-7}	48.46	1.27×10^{-5}	4.73

Table 5: Composite plate test case: extrapolation parameters for two *LSF* formulations at different M/N sample ratios ($N = 100$)

From such results, it is confirmed that the estimations of the extrapolation parameters ϕ_1, ϕ_2 and ξ_{12} do not depend on the sample size. For a same *LSF* formulation, mean values are not affected by the ratio M/N. On the other hand, bigger dataset sizes can improve ξ_{12} estimation precision, as can be seen in Table 5. Increasing ratio M/N can be used as an efficient procedure to enlarge the database by only enriching the population of the cheapest variable, thus without a huge additional computational burden. Moreover, from Table 5 it may be observed that the *LSF* formulation itself can greatly affect the average values of ϕ_2 and ξ_{12}: the former is increased, while ξ_{12} mean value decreases when switching from *LRVF* to *HRVF*.

Looking at ϕ_1 results, a remarkable difference in average values is obtained in the upper-mentioned formulations. However, this constitutes a second-order effect and thus does not significantly affect the final results in terms of variance of the estimation of P_f. The precision improvement provided by *HRVF* with respect to *LRVF* is thought to be circumstantial and just related to the adopted use case.

Estimations related to ξ_{12} seem poor in *LRVF* case: however, being on average two orders of magnitude lower than the others, their effect is not relevant. This excessive error is mostly due to the low magnitude of the quantity itself. A similar precision issue is also visible for ϕ_2 in *HRVF*, with the difference that here larger M/N ratios can reduce the related standard deviation.

Thanks to the upper-mentioned parameters, contour plots are extrapolated and reported in Fig. 2, where M number of R samples constitutes the abscissa, N number of S samples is the ordinate and the curves represents the ensemble of points allowing the same estimation precision, defined through the coefficient of variation $coV(\widehat{P_f})$. In such graphs, it is visible that every iso-coV can be described as an hyperbole branch. As shown in Section 3.3, all points minimizing the product NM are perfectly aligned in logarithmic axes, as the reference ratio does not depend on the targeted variance level. It is possible to recognize a vertical asymptote, identifying the minimum number M of R samples, and an horizontal one, related to minimum N. The reference ratio M/N described in Section 3.3 represents a transition between two asymptotic behaviors. Therefore, for ratios M/N higher than the reference one, precision will be defined essentially by N and adding further R samples would be ineffective. The opposite considerations can be done for ratios M/N lower than the reference one. The estimated value of such reference ratio M/N can be seen as a decision tool to state which component (namely R or S) mostly contributes to variance of $\widehat{P_f}$ estimation: in particular, if this is higher than 1, one can expect to improve precision by adding more R samples, and conversely if it is lower than 1. A sampling strategy can thus be defined from this ratio to reduce the number of samples, but it needs to be coupled with information about the relative computational burdens of R and S to make a more rational choice to reduce the overall analysis cost.

The effect of *LSF* formulation can be extrapolated from the translation towards right and down of the contour plots when transitioning from *LRVF* to *HRVF*. This implies that the minimum number N of response samples can be reduced, while the minimum number M of capacity samples and the reference ratio M/N are increased. Such phenomenon can be explained by the higher (respectively lower) variability assigned to R (respectively S) component in *HRVF*. Associating results from Eq. 27, Table 5 and Fig. 2, it can be observed that ξ_{12} translates coV contour plot horizontally (towards right as it increases), ϕ_2 is responsible for vertical translation (towards up if it increases) and ϕ_1 has a minor effect on the contour shape.

Another aspect to take into account is the variance reduction - measured in terms of $coV(\widehat{P_f})$ ratios - provided by ImpSMC with respect to IS, used as

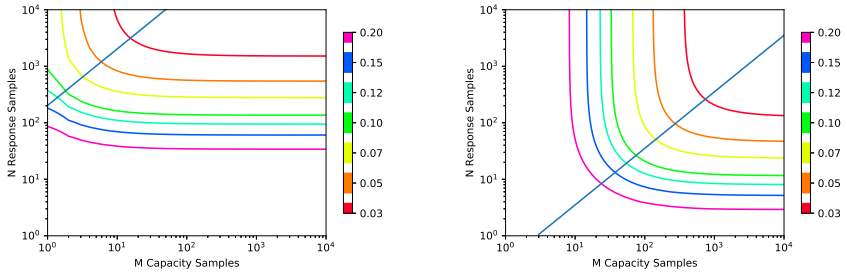

(a) *LRVF* (b) *HRVF*

Figure 2: Composite plate test case: $coV(\widehat{P_f})$ contour plots on two LSF formulations

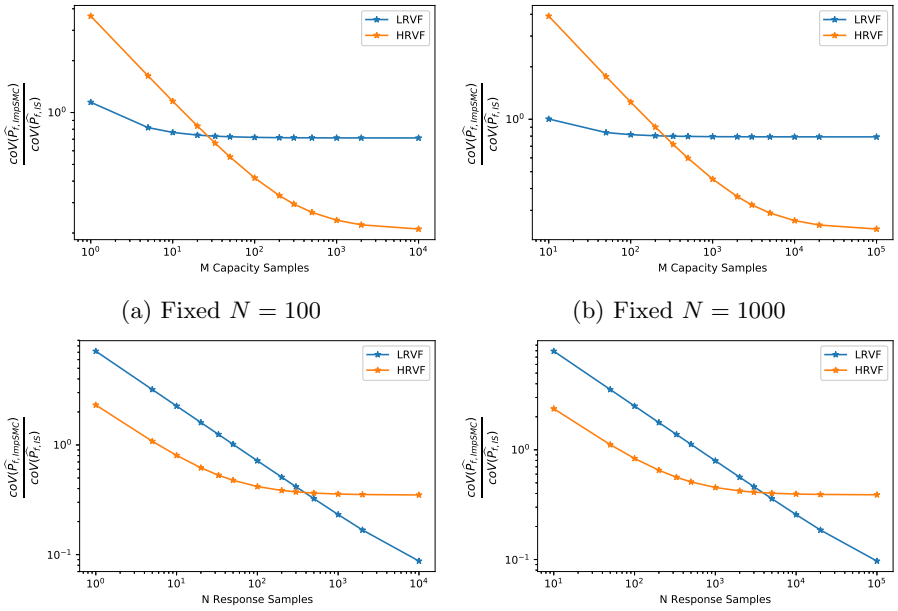

(a) Fixed $N = 100$ (b) Fixed $N = 1000$

(c) Fixed $M = 100$ (d) Fixed $M = 1000$

Figure 3: Composite plate test case: effect of LSF formulation on variance reduction of$\widehat{P_f}$ estimation as a function of number of samples N of S and M of R

reference. Relative results are extrapolated from variance estimator, as done for the $coV(\widehat{P_f})$ contour plots, and reported in Fig. 3. The simple introduction of a separated sampling approach on the same amount of data is given by the central abscissa point in every subplot (corresponding to $M/N = 1$): it can

be seen that in any case, substantial gains are ensured by ImpSMC approach, without even altering the ratio M/N.

For *LRVF*, N number of S samples has a significant impact on variance reduction, while little effect is observed from M number of R samples. The gains illustrated herein are in line with the ones reported in Table 3. These stem directly from the $coV(\widehat{P_f})$ contour plot. In fact, as for $M > 10$, only horizontal lines are present in Fig. 2a, the only relevant effect is provided by N. Such conclusions are confirmed when switching from Fig. 3a to 3b or from 3c to 3d.

Focusing on *HRVF*, both N and M significantly affect precision. They both have a nonlinear effect on variability of P_f estimation for small sample sizes, reaching an asymptotic behavior for bigger sizes. These observations are direct consequences of the contour plot in Fig. 2b: compared to *LRVF*, contours of the *HRVF* are more balanced and almost symmetric with respect to the first bisector of the Cartesian plane (in logarithmic axes). However, considering the reference ratio $M/N \approx 3$ (individuated by the hyperbole branch bisector), a slightly superior influence of M is expected. This is confirmed in Fig. 3, where a delay in transition from nonlinear to asymptotic behavior of M with respect to N can be observed by comparing Figs. 3a and 3c (or alternatively Figs. 3b and 3d): this implies that the increase of M keeps affecting precision at higher samples sizes than N does. As for *LRVF*, no difference is encountered in terms of variance reduction (with respect to IS) when increasing the overall database size without altering the ratio M/N, as it appears when comparing Fig. 3a with 3b or 3c with 3d.

Again, the differences between ImpSMC performances in *LRVF* and *HRVF* directly come from the $coV(\widehat{P_f})$ contour plots. Moreover, these do not depend on the size of the dataset itself but just on the adopted ratio M/N and *LSF* formulation. Variance reduction effects are directly reflected on the number of samples required to achieve a target precision.

4.2 Truss test case

In this section, we focus on a common benchmark problem, generally adopted as medium-complexity reliability example [Blatman & Sudret (2011), Lelievre (2018)], mainly due to a medium-large number of uncertain design variables. A 23-bar truss problem is considered (confront Fig. 4), for which the LSF is formulated here as:

$$g(V_{all}, X_S) = V_{all} - V_1(X_S) \tag{30}$$

Where X_S represents the whole set of variables affecting the deflection V_1, computed through Finite Element Analysis (FEA). Maximum allowable deflection is denoted as V_{all}. In this paper, we modify the problem by assigning different Young's Modulus and cross section areas to each finite element, with different section statistical distributions for horizontal and oblique bars. Considering 23 elements, 6 load variables and one capacity variable (the allowed V_{all}),

we have overall 53 random variables (52 forming X_S and one forming X_R). We use mean $\overline{S} = \overline{V_1} = 0.079$ and standard deviation $\sigma(S) = \sigma(V_1) = 6.47 \times 10^{-3}$ as references to analyze results from different configurations in following sections.

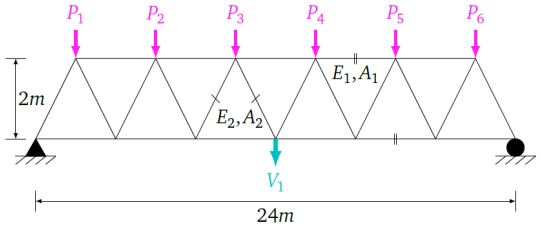

Figure 4: Truss test case: illustration (Source: Lelievre (2018))

Variable	**Unit**	**Distribution**	**Mean**	**St. Deviation**
E_1, E_2	GPa	Log-Normal	210	21
A_1	m^2	Log-Normal	2.0×10^{-3}	2.0×10^{-4}
A_2	m^2	Log-Normal	1.0×10^{-3}	1.0×10^{-4}
$P_1 - P_6$	N	Gumbel	5.0×10^4	7.5×10^3
V_{all}	m	Normal	0.115	0.01

Table 6: Truss test case: random variables

As done previously for the composite plate test case, several configurations of the truss example were used to experimentally validate the analytical variance estimators. The experimental validation is reported in Appendix A: in all configurations analyzed, the maximum error never exceeded 2%, while the mean value of errors was below 0.3%.

In Table 7, all main results related to different reliability estimators are provided, as done for the previous test case. Note that the mean, standard deviation and coV estimations of $\widehat{P_f}$ and required N to achieve $coV(\widehat{P_f}) = 0.05$ come from statistical repetition of 100 reliability analysis: the analytical variance estimator was used to stop sampling when target $coV = 0.05$ was obtained. Several ratios between number of sample N of S and M of R were introduced for both SMC and ImpSMC approaches. It can be easily observed that this latter allows to reduce both variance at fixed number N of response samples and necessary amount of simulations to achieve a fixed coV, clearly outperforming MC, IS and SMC. Moreover, such gains can be even improved by increasing the ratio M/N, then reaching an asymptotic behavior at very high M/N ratios.

As done for the previous numerical example, the $coV(\widehat{P_f})$ contour plot as a function of both N and M is plotted in Fig. 5, by using the algorithm described in Section 3.3.

Overall, 15 configurations are defined to take into account different variabilities of the capacity variable R. The correspondent means are calibrated

		Results at $coV(\widehat{P_f}) = 0.05$			**Results at** $N = 100$		**Results at** $N = 1000$	
		$\widehat{P_f}$	$\overline{N}$	σ_N (%)	$\sigma(\widehat{P_f})$	$coV(\widehat{P_f})$	$\sigma(\widehat{P_f})$	$coV(\widehat{P_f})$
MC		2.01×10^{-3}	2×10^5	5.46	4.21×10^{-3}	2.094	1.38×10^{-3}	0.687
IS		1.97×10^{-3}	1862	21.52	4.01×10^{-4}	0.204	1.32×10^{-4}	0.067
SMC	**M/N = 1**	1.98×10^{-3}	3.51×10^4	7.82	2.13×10^{-3}	1.077	5.15×10^{-4}	0.261
	M/N = 10	1.96×10^{-3}	1.33×10^4	14.05	1.17×10^{-3}	0.598	3.45×10^{-4}	0.176
	M/N = 100	1.96×10^{-3}	1.07×10^4	21.25	1.11×10^{-3}	0.568	3.41×10^{-4}	0.174
ImpSMC	**M/N = 1**	1.98×10^{-3}	190	41.79	1.47×10^{-4}	0.074	4.35×10^{-5}	0.022
	M/N = 10	1.96×10^{-3}	155	39.01	1.26×10^{-4}	0.064	3.83×10^{-5}	0.020
	M/N = 100	1.96×10^{-3}	150	33.66	1.23×10^{-4}	0.062	3.77×10^{-5}	0.019

Table 7: Truss test case: main reliability results from different simulation algorithms (values issued from 100 repetitions of each reliability algorithm)

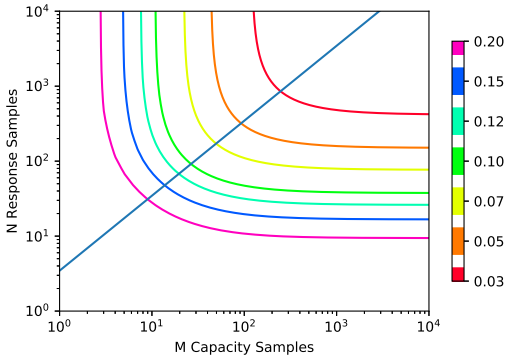

Figure 5: Truss nominal case: coV contour plot

to maintain the same failure probability target P_f of the nominal case. These are listed in Table 8 (ID=8 corresponds to nominal case). In this Section, all statistical parameters of S are kept constant: mean $\overline{S} = \overline{V_1} = 0.079$, standard deviation $\sigma(S) = \sigma(V_1) = 6.47 \times 10^{-3}$) and coefficient of variation $coV(S) = coV(V_1) = 0.082$. Reference results related to MC and IS are reported in Table 9.

A first evaluation can be done with respect to different evolutions shown in the coV contour plots, depicted in Fig. 6. The reader may observe a translation toward down-right of the contours as the ratio $\sigma(R)/\sigma(S)$ increases (Fig. 6b). This implies that the necessary number of needed M samples increases, while minimum N decreases. The reference ratio M/N will therefore increase. It is worth noticing that in this case, as $N > 10$, the dominant contributor to the P_f estimate precision will be M, as we are already very close to the vertical asymptote. Opposite conclusions are drawn if the ratio $\sigma(R)/\sigma(S)$ is reduced (Fig. 6a).

Another aspect to consider is the variance reduction allowed by ImpSMC approach with respect to N and M. In the previous section it was already observed the potential variance reduction (compared to other reliability simulation-base algorithms) for a nominal case and with different N and M/N ratios. In Fig.

ID	$\overline{R}$	$\sigma(R)$	$coV(R)$	$\overline{R}/\overline{S}$	$\sigma(R)/\sigma(S)$	$coV(R)/coV(S)$
1	0.1023	0.001	0.01	1.29	0.16	0.12
2	0.1024	0.0012	0.012	1.30	0.19	0.15
3	0.1026	0.0016	0.016	1.30	0.25	0.20
4	0.1028	0.002	0.019	1.30	0.30	0.23
5	0.1031	0.0025	0.024	1.31	0.38	0.29
6	0.1037	0.0033	0.032	1.31	0.51	0.39
7	0.1057	0.005	0.047	1.34	0.77	0.57
8*	0.115	0.01	0.087	1.46	1.55	1.06
9	0.1405	0.02	0.142	1.78	3.08	1.73
10	0.1685	0.03	0.178	2.13	4.64	2.17
11	0.196	0.04	0.204	2.48	6.18	2.49
12	0.225	0.05	0.222	2.85	7.72	2.71
13	0.253	0.06	0.237	3.20	9.27	2.89
14	0.31	0.08	0.258	3.92	12.36	3.15
15	0.368	0.10	0.272	4.66	15.46	3.32

Table 8: Truss test case: configurations for study on $\sigma(R)/\sigma(S)$ effect (fixed statistical parameters of S: mean $\overline{S} = \overline{V_1} = 0.079$, standard deviation $\sigma(S) = \sigma(V_1) = 6.47 \times 10^{-3}$ and coefficient of variation $coV(S) = coV(V_1) = 0.082$)

ID	$\sigma(R)/\sigma(S)$	MC			IS		
		$\widehat{P_f}$	$\overline{N}$	$\sigma_N/\overline{N}(\%)$	$\widehat{P_f}$	$\overline{N}$	$\sigma_N/\overline{N}(\%)$
1	0.16	1.91×10^{-3}	2.10×10^5	5.23	1.91×10^{-3}	3351	37.8
2	0.19	1.90×10^{-3}	2.11×10^5	4.45	1.95×10^{-3}	3289	49.2
3	0.25	1.93×10^{-3}	2.08×10^5	4.72	1.88×10^{-3}	3154	31.7
4	0.30	1.91×10^{-3}	2.10×10^5	4.73	1.97×10^{-3}	3376	38.2
5	0.38	1.90×10^{-3}	2.11×10^5	5.00	1.88×10^{-3}	3309	73.2
6	0.51	1.97×10^{-3}	2.03×10^5	5.06	1.91×10^{-3}	2927	29.6
7	0.77	1.96×10^{-3}	2.04×10^5	4.77	1.98×10^{-3}	2643	31.0
8*	1.55	1.98×10^{-3}	2.03×10^5	5.27	2.08×10^{-3}	1868	20.7
9	3.08	1.93×10^{-3}	2.08×10^5	4.37	1.98×10^{-3}	1399	16.0
10	4.64	1.87×10^{-3}	2.14×10^5	5.17	1.87×10^{-3}	1353	5.2
11	6.18	2.02×10^{-3}	1.98×10^5	4.76	2.02×10^{-3}	1298	11.3
12	7.72	1.95×10^{-3}	2.05×10^5	5.43	1.94×10^{-3}	1317	5.1
13	9.27	2.02×10^{-3}	1.98×10^5	4.94	2.01×10^{-3}	1282	11.4
14	12.36	2.03×10^{-3}	1.97×10^5	5.21	2.16×10^{-3}	1275	15.2
15	15.46	2.00×10^{-3}	2.01×10^5	5.55	2.02×10^{-3}	1286	11.6

Table 9: Truss test case: reference results for study on $\sigma(R)/\sigma(S)$ effect (100 simulations considered, targeted $coV(\widehat{P_f}) = 0.05$)

7 is reported a complete study over the effects of the ratio $\sigma(R)/\sigma(S)$. Results are consistent with previous conclusions from contour plots. All curves related to configurations with $\sigma(R) \ll \sigma(S)$ show a small sensitivity to variations of M, but a massive coV reduction can be achieved by increasing N. With the increase of the ratio $\sigma(R)/\sigma(S)$, impact of M over coV becomes more visible, while the influence of N is reduced. The turning point is given by $\sigma(R) \approx \sigma(S)$, where the effects of N and M are almost perfectly balanced. Then, for $\sigma(R) \gg \sigma(S)$, the only responsible for coV is the number M of R samples. Comparing ImpSMC and IS performances, the coV reduction factor is kept constant when multiplying

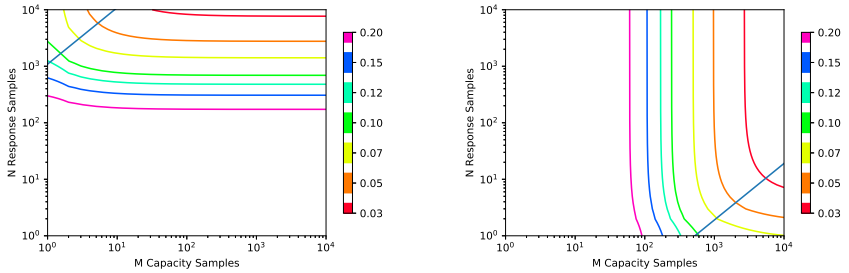

(a) $\sigma(R) = 0.001$, $\frac{\sigma(R)}{\sigma(S)} = 0.155$ (b) $\sigma(R) = 0.1$, $\frac{\sigma(R)}{\sigma(S)} = 15.5$

Figure 6: Truss test case: effect of $\sigma(R)/\sigma(S)$ on coV contour plot

the available computational budget: this is visible when passing from $N = 100$ (respectively $M = 100$) to $N = 1000$ (respectively $M = 1000$) we obtain almost identical graphs of coV_{ImpSMC}/coV_{IS}.

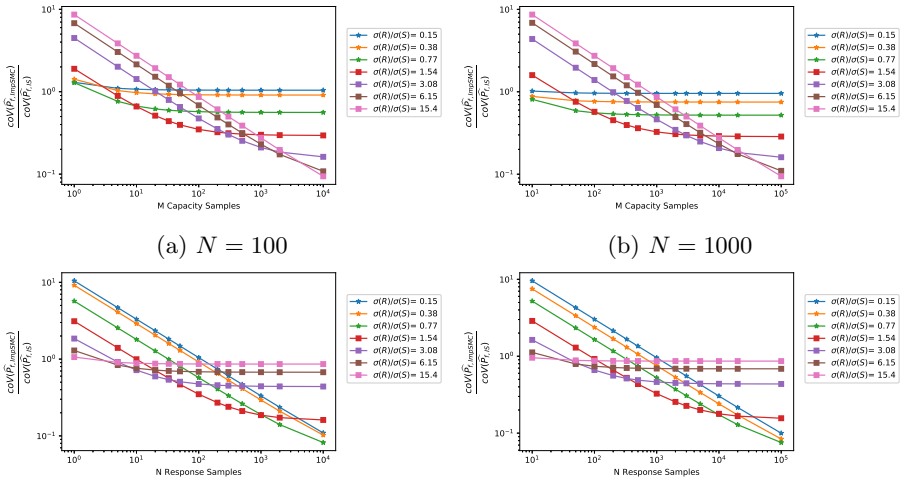

(a) $N = 100$ (b) $N = 1000$

(c) $M = 100$ (d) $M = 1000$

Figure 7: Truss test case: effect of $\sigma(R)/\sigma(S)$ on variance reduction in function of number of samples N of S and M of R (fixed $\sigma(S) = 6.47 \times 10^{-3}$)

We would now like to make some comments regarding the computational cost gains. Thanks to the variance estimator, it is in fact also possible to preview the overall number of complete analysis without even needing to actually perform them.

In Fig. 8, attention is focused on the balance of necessary N (as in this example, response sampling is computationally more expensive than capacity) to achieve a target $coV = 0.05$. This analysis allows to confirm what was

previewed in previous sections. In fact, when $\sigma(R) < \sigma(S)$ the effect of M/N is not relevant, and ImpSMC approaches IS when $\sigma(R) \ll \sigma(S)$. On the other hand, when $\sigma(R) \gg \sigma(S)$, low ratios M/N do not allow to fully exploit ImpSMC potentialities, as the necessary M increases. In this context, it is fundamental to increase the imposed ratio M/N to be able to decrease N (which is usually the main contributor to overall computational burden).

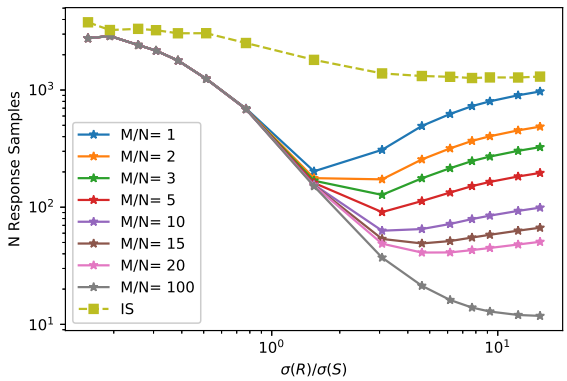

Figure 8: Truss test case: effect of $\sigma(R)/\sigma(S)$ on needed number of samples N of S and M of R to achieve $cov(P_f) = 0.05$ at given M/N ratios

5 Discussion of results

From the analysis conducted in the two test cases some general conclusions can be drawn.

First, the only assumption for the formalization of the ImpSMC approach relies on the possibility of separating LSF in two independent variables R and S: therefore, no further assumption on the shape of LSF nor the operation linking R and S is needed. Additionally, ImpSMC approach can be applied to any engineering field and extended to system reliability applications, aerodynamic studies, power engineering or even fields outside of engineering requiring the determination of a reliability, like pharmaceutic industry.

From the study on the composite plate, it can be observed that slight changes in LSF formulation can lead to substantial gains. The key point in transferring - whenever possible - variability on the computationally cheapest component (between response and capacity) can allow to reduce the needed amount of samples required to achieve a prescribed precision target, above all when making use of unbalanced datasets.

From both test cases, we observed that the efficiency of increasing ratio M/N is more relevant with high levels of the ratio $\sigma(R)/\sigma(S)$. This is valid for all situations where response sampling implies a fairly superior computational

burden, compared to capacity sampling. This means that in such cases, if the variability of the capacity R is greater than that of response S, more capacity samples (M) can be very efficiently generated and allow to significantly decrease the variability of the P_f estimate. The reverse reasoning must be done in the opposite situation, where most of computational efforts comes from resistance model.

In industrial engineering applications, such an analytical variance estimator can predict the precision of failure probability estimation and the required amount of simulations to achieve a good precision target without being forced to replicate empirically the entire procedure for a statistical analysis. Moreover, the bisector of the $coV(\widehat{P_f})$ plot (which can be estimated from a low number of samples) may give an idea of a good ratio M/N between number of capacity and response samples to guarantee a good compromise between precision and computational burden. However, as this just minimizes the product NM, engineering judgment is needed to refine it: if sampling the response S is more expensive than sampling capacity R, this ratio can be multiplied - or divided, if the reverse consideration is valid - up to 10 (no more than this as an asymptotic behavior would be reached).

6 Conclusion

In this paper, an analytical variance estimator related to ImpSMC approach is proposed and numerical studies are conducted on two test cases. This method can be used to estimate failure probability in reliability applications where it is possible to identify two separated independent components in the Limit State Function (LSF). Generally, we could think of response and capacity of a system. In structural applications, we refer respectively to stress and strength.

The basic idea of ImpSMC is to separately sample these two components and concentrate them around failure zones. Thanks to the variance estimator, it is possible to show without large number of simulations how such an approach outperforms other simulation methods like MC, IS and SMC. Variance of the P_f estimator is significantly reduced as well as the number of required samples to achieve a good precision target. Separate sampling also allows to deal with unbalanced datasets, leading to even higher gains. Results show that ImpSMC approaches IS when all variability in LSF comes from the most expensive component. In all other cases, precision improvements with respect to IS are significant, above all in the opposite situation of variability mostly due to the cheapest component of LSF.

The two test cases presented in this paper, despite their simplicity, allow to highlight the potential of a variance estimator for ImpSMC. In particular, the first use case shows that it is not an obligation to distinguish a stress and a strength component, but LSF can be re-adapted (if possible) to any form containing two separated independent terms. A key to increase gains in term of computational burden is to work towards unbalanced datasets and assigning (where possible) most of variability to the component which is cheaper to

sample.

Focusing on the practical use of ImpSMC approach, the allowance of unbalanced datasets is of utmost importance. Generally, the response S of a system is often much more expensive to sample than the capacity R: for example, in structural applications, the response will be provided by finite element model simulations, while the capacity is often given by an empirically characterized random variable which is cheap to sample. Allowing unbalanced datasets, one can focus on maximizing the ratio between the number M of R samples and the number N of S samples to reduce the overall computational burden, while improving the precision of the estimation of the failure probability P_f.

Moreover, coupling our method to Adaptive Importance Sampling algorithm could extend its application to any reliability problem with unknown importance function.

Finally, the introduction of ImpSMC in machine learning techniques would make it possible to cheaply evaluate failure probability in real-life applications where response is so expensive to evaluate that it must be approximated by a surrogate model.

References

Au, S.-K. & Beck, J. L. (1999), 'A new adaptive importance sampling scheme for reliability calculations', *Structural safety* **21**(2), 135–158.

Birolini, A. (2013), *Reliability engineering: theory and practice*, Springer Science & Business Media.

Blatman, G. & Sudret, B. (2011), 'Adaptive sparse polynomial chaos expansion based on least angle regression', *Journal of computational Physics* **230**(6), 2345–2367.

Cappé, O., Douc, R., Guillin, A., Marin, J.-M. & Robert, C. P. (2008), 'Adaptive importance sampling in general mixture classes', *Statistics and Computing* **18**(4), 447–459.

Chaudhuri, A. & Haftka, R. T. (2013), 'Separable monte carlo combined with importance sampling for variance reduction', *International Journal of Reliability and Safety* **7**(3), 201–215.

Chaudhuri, A., Kramer, B. & Willcox, K. E. (2020), 'Information Reuse for Importance Sampling in Reliability-Based Design Optimization', *Reliability Engineering & System Safety* **201**, 106853.

De Rocquigny, E., Devictor, N., Tarantola, S., Lefebvre, Y., Pérot, N., Castaings, W., Mangeant, F., Schwob, C., Lavin, R., Masse, J.-R., Limbourg, P., Kanning, W. & Gelder, P. (2008), 'Uncertainty in industrial practice: A guide to quantitative uncertainty management'.

Gao, H., Wang, A., Zio, E. & Bai, G. (2020), 'An integrated reliability approach with improved importance sampling for low-cycle fatigue damage prediction of turbine disks', *Reliability Engineering & System Safety* **199**, 106819.

Gogu, C. (2021), *Mechanical Engineering under Uncertainties: From Classical Approaches to Some Recent Developments*, ISTE-Wiley.

Hammersley, J. (2013), *Monte carlo methods*, Springer Science & Business Media.

Hasofer, A. M. & Lind, N. C. (1974), 'Exact and invariant second-moment code format', *Journal of the Engineering Mechanics division* **100**(1), 111–121.

Karamchandani, A., Bjerager, P. & Cornell, C. (1989), Adaptive importance sampling, *in* 'Structural Safety and Reliability', ASCE, pp. 855–862.

Larsson, O. (2015), 'Reliability analysis', *Lecture notes, Lund University*.

Lelievre, N. (2018), Développement des méthodes AK pour l'analyse de fiabilité. Focus sur les évènements rares et la grande dimension, PhD thesis, Université Clermont Auvergne.

Lemaire, M. (2013), *Structural reliability*, John Wiley & Sons.

Liu, F., Wei, P., He, P. & Dai, Y. (2022), 'Application of an improved sequential importance sampling for structural reliability analysis of aeronautical hydraulic pipeline with multiple stochastic responses', *Structural and Multidisciplinary Optimization* **65**(2), 1–14.

Misraji, M. A., Valdebenito, M. A., Jensen, H. A. & Mayorga, C. F. (2020), 'Application of directional importance sampling for estimation of first excursion probabilities of linear structural systems subject to stochastic gaussian loading', *Mechanical Systems and Signal Processing* **139**, 106621.

Müller, T., McWilliams, B., Rousselle, F., Gross, M. & Novák, J. (2019), 'Neural importance sampling', *ACM Transactions on Graphics (TOG)* **38**(5), 1–19.

Nadjafi, M. & Najafi ARK, A. (2021), 'Improving accuracy in importance sampling: An integrated approach with fuzzy-strata sampling', *International Journal of Reliability, Risk and Safety: Theory and Application* **4**(1), 61–67.

Nikolaidis, E., Ghiocel, D. M. & Singhal, S. (2007), *Engineering design reliability applications: for the aerospace, automotive and ship industries*, CRC Press.

Papaioannou, I., Geyer, S. & Straub, D. (2019), 'Improved cross entropy-based importance sampling with a flexible mixture model', *Reliability Engineering & System Safety* **191**, 106564.

Pham, H. (2006), *Handbook of reliability engineering*, Springer Science & Business Media.

Rausand, M. & Høyland, A. (2003), *System reliability theory: models, statistical methods, and applications*, Vol. 396, John Wiley & Sons.

Richard, J.-F. & Zhang, W. (2007), 'Efficient high-dimensional importance sampling', *Journal of Econometrics* **141**(2), 1385–1411.

Rykov, V. V., Balakrishnan, N. & Nikulin, M. S. (2010), *Mathematical and Statistical Models and Methods in Reliability: Applications to Medicine, Finance, and Quality Control*, Springer Science & Business Media.

Saaed, A. & Daghigh, M. (2021), 'Dynamic reliability analysis of moment resisting concrete frames', *International Journal of Reliability, Risk and Safety: Theory and Application* **4**(1), 17–22.

Smarslok, B. P. (2009), 'Measuring, using, and reducing experimental and computational uncertainty in reliability analysis of composite laminates', *Ph. D. Thesis*.

Smarslok, B. P., Haftka, R. T., Carraro, L. & Ginsbourger, D. (2010), 'Improving accuracy of failure probability estimates with separable monte carlo', *International Journal of Reliability and Safety* **4**(4), 393–414.

Subramanian, A. & Mahadevan, S. (2022), 'Importance sampling for probabilistic prognosis of sector-wide flight separation safety', *Reliability Engineering & System Safety* **222**, 108410.

Tabandeh, A., Jia, G. & Gardoni, P. (2022), 'A review and assessment of importance sampling methods for reliability analysis', *Structural Safety* **97**, 102216.

Tokdar, S. T. & Kass, R. E. (2010), 'Importance sampling: a review', *Wiley Interdisciplinary Reviews: Computational Statistics* **2**(1), 54–60.

Trivedi, K. S. & Bobbio, A. (2017), *Reliability and availability engineering: modeling, analysis, and applications*, Cambridge University Press.

Zhang, P. (1996), 'Nonparametric importance sampling', *Journal of the American Statistical Association* **91**(435), 1245–1253.

Zhang, X., Lu, Z. & Cheng, K. (2022), 'Cross-entropy-based directional importance sampling with von Mises-Fisher mixture model for reliability analysis', *Reliability Engineering & System Safety* **220**, 108306.

A Experimental variance validation on truss test case

ID	M/N=1			M/N=10			M/N=100		
	$\sigma_{emp}(P_f)$	$\sigma_{an}(P_f)$	$Err(P_f)(\%)$	$\sigma_{emp}(P_f)$	$\sigma_{an}(P_f)$	$Err(P_f)(\%)$	$\sigma_{emp}(P_f)$	$\sigma_{an}(P_f)$	$Err(P_f)(\%)$
1	1.966×10^{-4}	1.958×10^{-4}	-0.39	1.680×10^{-4}	1.673×10^{-4}	-0.39	1.593×10^{-4}	1.586×10^{-4}	-0.46
7	8.615×10^{-5}	8.549×10^{-5}	-0.77	8.482×10^{-5}	8.515×10^{-5}	0.38	8.480×10^{-5}	8.514×10^{-5}	
8	4.331×10^{-5}	4.345×10^{-5}	0.31	3.827×10^{-5}	3.838×10^{-5}	0.29	3.779×10^{-5}	3.765×10^{-5}	-0.38
12	8.302×10^{-5}	8.304×10^{-5}	0.02	2.666×10^{-5}	2.709×10^{-5}	1.60	1.084×10^{-5}	1.081×10^{-5}	-0.28
15	9.868×10^{-5}	9.827×10^{-5}	-0.41	3.139×10^{-5}	3.138×10^{-5}	-0.39	1.041×10^{-5}	1.042×10^{-5}	0.10

Table 10: Truss test case: validation of analytical variance estimator (configurations ID from Table 8, $N = 10^3$, values issued from 10^5 repetitions)